Distinct Difference in Ionic Transport Behavior in Polymer Electrolytes Depending on the Matrix Polymers and Incorporated Salts

Shiro Seki, Md. Abu Bin Hasan Susan,† Taketo Kaneko, Hiroyuki Tokuda, Akihiro Noda, and Masayoshi Watanabe*

Department of Chemistry and Biotechnology, Yokohama National University and CREST-JST, 79-5 Tokiwadai, Hodogaya-ku, Yokohama 240-8501, Japan

Received: October 13, 2004; In Final Form: January 10, 2005

Two different electrolyte salts, lithium bis(trifluoromethanesulfonyl)imide (LiTFSI), and a room temperature ionic liquid, 1-ethyl-3-methylimidazolium bis(trifluoromethanesulfonyl)imide (EMITFSI), were incorporated into network polymers to obtain ion-conductive polymer electrolytes. Network polymers of poly(ethylene oxide-*co*-propylene oxide) (P(EO/PO)) and poly(methyl methacrylate) (PMMA) were chosen as matrixes for LiTFSI and EMITFSI, respectively. Both of the polymer electrolytes were single-phase materials and were completely amorphous. Ionic conductivity of the polymer electrolytes was measured over a wide temperature range, with the lowest temperatures close to or below the glass transition temperatures (T_g). The Arrhenius plots of the conductivity for both of the systems exhibited positively curved profiles and could be well fit to the Vogel−Tamman−Fulcher (VTF) equation. The conductivity of the PMMA/EMITFSI electrolytes was higher at most by 3 orders of magnitude than that of the LiTFSI/P(EO/ PO) electrolytes at ambient temperature. When the ideal glass transition temperature, T_0 (one of the VTF fitting parameters), was compared with the T_g, a difference in the ionic conduction was apparent in these systems. In the P(EO/PO)/LiTFSI electrolytes, the T_0 and T_g increased in parallel with salt concentration and the T_0 was lower than the T_g by ca. 50 °C. On the contrary, the difference between the T_0 and the T_g increased with increasing content of PMMA in the PMMA/EMITFSI electrolytes, with the observed difference in the concentration range studied reaching up to ca. 100 °C. The conductivity at the T_g, $\sigma(T_g)$, for the LiTFSI/P(EO/PO) electrolytes was on the order of 10^{-14}−10^{-13} S cm^{-1} and increased with increasing salt concentration, whereas that for the PMMA/EMITFSI polymer electrolytes reached 10^{-7} S cm^{-1} when the concentration of PMMA was high. The ion transport mechanism was discussed in terms of the concepts of *coupling*/*decoupling* and *strong*/*fragile* for the two different polymer electrolytes.

Introduction

Polymer electrolytes have been recognized as the most viable electrolytes for potential application in a wide variety of solid-state electrochemical devices.[1] Conventional electrolytes of this variety, typically polyether-based polymer electrolytes, are solid solutions of electrolyte salts in polymers. The ionic motion in these electrolytes, known widely as salt-in-polymer electrolytes, is coupled with the local segmental motion.[2,3] This system is recognized as a *coupled* system, and the conduction relaxation time is coupled with the relaxation time for the segmental motion of the polymer matrix. Molecular design to achieve fast ion transport in such a system has been based on the preparation of polyethers having low glass transition temperatures (T_g) and having hyperbranched structures to utilize the fast molecular motion of the ion-coordinating side chains for the ionic transport.[4] Although these methodologies are effective to increase ionic conductivity to some extent, the conductivity values at ambient temperature are still much lower than those of common aprotic electrolyte solutions. The meager conductivity can partly be attributed to the fact that the generation of carrier ions occurs via the interaction of polymer segments and ions, and increases in the carrier ion density and mobility are inconsistent. A decrease in the ionic mobility caused by the suppression of the polymer dynamics, which is reflected in an increase in the T_g, offsets the effect of increasing carrier ion density with increasing ionic concentration.

In contrast, the use of high salt concentrations (exceeding 50 wt %) has been successfully demonstrated for the preparation of polymer-in-salt systems.[5,6] A small amount of high-molecular-weight polymers suffices to give rubbery compliance with high ionic conductivity for certain polymer-in-salt systems. The electrolyte salts for such a polymer-in-salt system need to have some essential characteristics, such as low T_g and melting temperature (T_m), and to be (supercooled) liquids at ambient temperature, while retaining high ionic conductivity and compatibility with host polymers. Consequently, high ionic conductivity at ambient temperature that is not coupled with the segmental motion of the polymers might be achieved, where the conduction relaxation time is decoupled from and is much faster than the structural relaxation time.

Possible electrolyte salts for the polymer-in-salt system are room temperature molten salts, i.e., ionic liquids. Ionic liquids possess unique physicochemical properties, such as immeasurably low vapor pressure, high ionic conductivity, nonflamma-

* To whom correspondence should be addressed. E-mail: mwatanab@ynu.ac.jp. Phone/fax: +81-45-339-3955.

† Present address. Department of Chemistry, University of Dhaka, Dhaka-1000, Bangladesh.

10.1021/jp045328j CCC: $30.25
Published on Web 02/12/2005

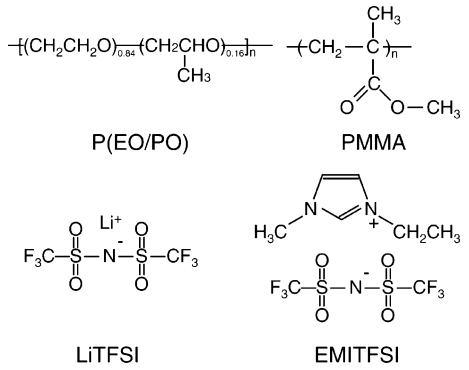

Figure 1. Structures of matrix polymers and electrolyte salts.

bility, and greater thermal and electrochemical stability,[7−9] and thereby meet the requirements of plasticizing salts. Furthermore, ionic liquids offer the potential for improved thermal and mechanical properties, and may expand the temperature range where flexible polymers can be used. We have already reported that polymer-in-salt electrolytes, prepared by dissolving compatible polymers in both chloroaluminate[10] and non-chloroaluminate[11] molten salts, exhibit high ionic conductivity as well as the rubbery electrolyte property. The ionic liquids based on imidazolium salts have been found to serve as excellent plasticizers for poly(methyl methacrylate) (PMMA) with improved thermal stability and ability to significantly reduce the glass transition temperatures.[12] Highly ion conducting rubbery gel electrolytes from non-chloroaluminate ionic liquids and poly(vinylidene fluoride-*co*-hexafluoropropylene) have also been reported by Carlin and co-workers.[13] In a recent paper, we have reported a new methodology affording highly conductive polymer electrolytes by in situ radical polymerization of vinyl monomers in ionic liquids.[14] Like conventional polymer gels, the obtained polymer electrolytes are comprised of polymer networks and liquids, ionic liquid in our case. If the incorporation of ionic liquid into polymer networks affords a completely compatible combination, we name the polymer gels obtained in this way "ion gels",[14−15] which are distinctly discriminated from conventional polymer gels in terms of their nonvolatility and high thermal stability. Since task-oriented properties, such as proton conduction, lithium ion conduction, and electron transport, can be molecularly designed into the ionic liquids, the scope and the utility of the ion gels as new polymer electrolytes will immediately expand to fuel cells,[16] lithium batteries,[17] and solar cells.[18]

We report here a systematic study to understand ion transport behavior in polymers and compare and contrast the physicochemical processes involved in ion gels with those for conventional polyether electrolytes in pursuit of a new molecular design of polymer electrolytes. In this study, we use ion gels obtained by the incorporation of 1-ethyl-3-methylimidazolium bis(trifluoromethanesulfonyl)imide (EMITFSI) in a hard matrix, PMMA, and conventional polymer electrolytes of lithium bis(trifluoromethanesulfonyl)imide (LiTFSI) incorporated into a soft matrix, poly(ethylene oxide-*co*-propylene oxide) (P(EO/PO)) (Figure 1). As mentioned, most of the studies on polymer electrolytes to date use poly(ethylene oxide) (PEO) and its derivatives as matrix polymers, and a lithium salt is dissolved in the matrix. Thus, the P(EO/PO)/LiTFSI system represents a conventional polymer electrolyte. On the other hand, incorporation of EMITFSI into the PMMA network has been found to afford a completely compatible combination,[14] and the behavior of ion gels seems to be best depicted in the PMMA/EMITFSI system compared with other network polymer systems. Although the two polymer electrolytes consist of very different salts and matrix polymers, both electrolytes are single-phase materials and are completely amorphous, which allows us to quantitatively compare the ion transport properties. With the aid of the calorimetric and conductometric results, we aim at clearly understanding the factors governing ionic transport in polymer electrolytes in terms of the concepts of *coupling*/*decoupling*[19−22] and *strong*/*fragile*.[20−23]

Experimental Section

Synthesis of EMITFSI. EMITFSI was synthesized following the procedure reported earlier.[14,24] The structure was identified by the melting point and ^{1}H NMR and FAB-mass spectra. The purified EMITFSI was stored in an argon atmosphere glovebox (VAC, $[O_2] < 1$ ppm, $[H_2O] < 1$ ppm).

Preparation of Polymer Electrolytes. The P(EO/PO)/LiTFSI polymer electrolytes were prepared by the photoinitiated polymerization[25a] using 2,2-dimethoxy-2-phenylacetophenone (DMPA) as a photoinitiator. A network polymer from P(EO/PO) triacrylate macromonomer[25b] (number average molecular weight $M_n = 8000$, kindly supplied by Dai-ichi Kogyo Seiyaku Co.) was used as the matrix of LiTFSI. LiTFSI and DMPA (0.1 wt % based on the macromonomer) were added to a mixture of the P(EO/PO) macromonomer and acetonitrile to form a homogeneous solution. The solution was then spread between two glass plates separated by poly(tetrafluoroethylene) spacers (Teflon, 0.2 mm in thickness) and irradiated with UV light for the cross-linking reaction of the macromonomers, and was then dried under vacuum for 24 h to completely remove acetonitrile. This yielded a transparent and self-standing polymer electrolyte.

The preparation of PMMA/EMITFSI polymer electrolytes has already been reported.[14] Deoxygenated MMA, ethylene glycol dimethacrylate (EGDMA; 2 mol % based on MMA), and benzoyl peroxide (BPO; 2 mol % based on MMA) as an initiator were dissolved in EMITFSI. The mixtures were spread between two glass plates separated by Teflon spacers (0.2 mm in thickness), and in situ free radical polymerization was conducted at 80 °C for 24 h, followed by heat treatment at 140 °C for 30 min to complete the polymerization, to obtain transparent and self-standing polymer electrolytes.

Salt concentration in these polymer electrolytes was normalized by dividing the number of moles of the salt by the total mass of the polymer electrolyte (mol kg^{-1}).

Differential Scanning Calorimetric Measurements. Differential scanning calorimetry (DSC) was carried out on a Seiko Instruments DSC 220C under a N_2 atmosphere. The samples for DSC measurements were tightly sealed in Al pans in the dry glovebox. The measurements for LiTFSI/P(EO/PO) systems were conducted with the samples heated to 100 °C, followed by cooling to −150 °C, and then heating again to 100 °C at a cooling and heating rate of 10 °C min^{-1}. The DSC thermograms for PMMA/EMITFSI systems, on the other hand, were recorded during cooling from 200 to −150 °C, followed by heating to 200 °C at a cooling and heating rate of 10 °C min^{-1}. The T_g (onset temperature of the heat capacity change) and T_m (onset temperature of the endothermic peak) were determined from DSC thermograms during the programmed reheating steps.

Ionic Conductivity Measurements. The ionic conductivity (σ) was measured in a hermetical cell by means of complex impedance measurements in the temperature range of −65 to +130 °C. The polymer electrolyte films were cut into disks of 13 mm diameter and then were sandwiched between mirror-finished stainless steel blocking electrodes. The measurements were conducted under controlled temperatures with cooling. For

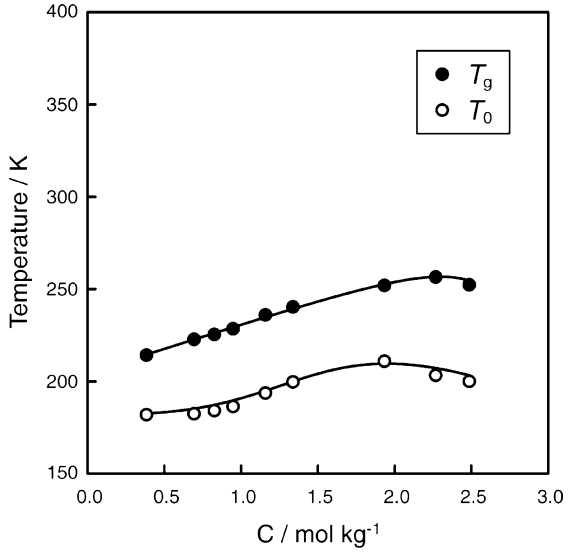

Figure 2. Glass transition temperature (T_g) and the ideal glass transition temperature (T_0) calculated from the VTF equation for P(EO/PO) network polymers containing LiTFSI as a function of LiTFSI concentration.

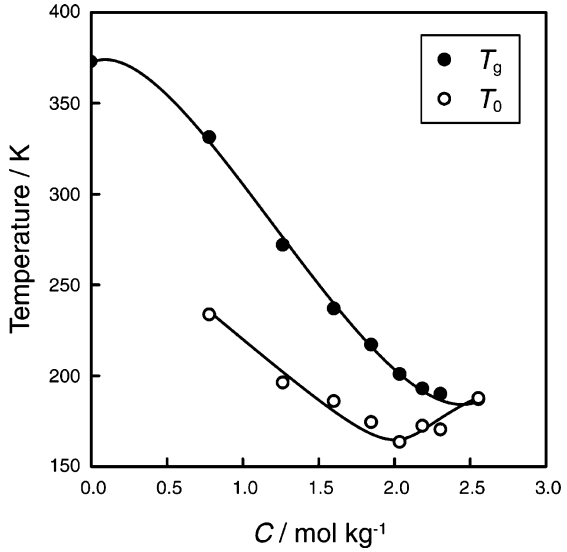

Figure 3. Glass transition temperature (T_g) and the ideal glass transition temperature (T_0) calculated from the VTF equation for PMMA network polymers with dissolved EMITFSI as a function of EMITFSI concentration.

TABLE 1: VTF Equation ($\sigma = AT^{-1/2}\exp[-B/(T - T_0)]$) Parameters for Ionic Conductivity Data and Glass Transition Temperatures for P(EO/PO)/LiTFSI Electrolytes

concn/ mol kg^{-1}	A/ S m^{-1} K$^{1/2}$	B/ 10^3 K	T_0/ 10^2 K	$10R^2$	T_g/ 10^2 K
0.386	0.117	0.857	1.82	9.99	2.14
0.696	0.489	1.03	1.82	9.99	2.23
0.828	0.280	1.00	1.84	9.99	2.25
0.949	0.634	1.04	1.86	9.99	2.28
1.16	0.614	1.02	1.94	9.99	2.36
1.34	0.721	1.00	2.00	9.99	2.40
1.93	0.730	1.04	2.11	9.99	2.52
2.27	2.61	1.30	2.03	9.99	2.56
2.49	3.33	1.47	2.00	9.99	2.52

TABLE 2: VTF Equation ($\sigma = AT^{-1/2}\exp[-B/(T - T_0)]$) Parameters for Ionic Conductivity Data and Glass Transition Temperatures for PMMA/EMITFSI Electrolytes

concn/ mol kg^{-1}	A/ S m^{-1} K$^{1/2}$	B/ 10^3 K	T_0/ 10^2 K	$10R^2$	T_g/ 10^2 K
0.777	5.00	1.45	2.34	9.99	3.31
1.26	8.51	1.25	1.96	9.99	2.72
1.60	2.76	0.806	1.85	9.99	2.37
1.85	5.89	0.825	1.74	9.99	2.17
2.04	11.0	0.790	1.69	9.99	2.01
2.18	8.24	0.655	1.70	9.99	1.93
2.30	13.4	0.734	1.62	9.99	1.90
2.56	4.54	0.428	1.83	9.99	1.87

the measurements in the high-temperature range (20−130 °C), a computer-controlled Hewlett-Packard 4192A LF impedance analyzer was used over the frequency range from 5 Hz to 1 MHz, while the measurements at low temperatures (−65 to +20 °C) were conducted on a computer-interfaced Solartron 1287 frequency response analyzer with a Keithley model 428 current amplifier over the frequency range from 10 μHz to 1 MHz. The samples were thermally equilibrated at each temperature for at least 1 h prior to the measurements.

Results and Discussion

Thermal Properties. Thermal properties of the polymer electrolyte systems were studied using DSC. DSC thermograms of the P(EO/PO)/LiTFSI electrolytes with varying LiTFSI concentration are shown in the Supporting Information, 1. In the concentration range studied, all the polymer electrolytes were completely amorphous, and only one T_g could be observed. Despite the high degree of crystallinity of poly(ethylene oxide), the introduction of a propylene oxide (PO) unit in the network suppressed crystallization of the polymer electrolytes. For all of the concentrations, the temperature range for the glass transition was quite narrow. The magnitude of the total heat capacity change corresponding to the glass transition decreases with increasing LiTFSI concentration.

Figure 2 shows the T_g of the polymer electrolytes, determined by DSC, as a function of lithium salt concentration in the P(EO/PO) network. The results have also been tabulated in Table 1. The T_g increases almost linearly with increasing salt concentration until it reaches a value of 1.93 mol kg^{-1} ([Li]/[O] = 0.20). At the higher concentrations of LiTFSI, the increase in the T_g becomes less pronounced. The coordination number of lithium cation with oxygen atoms of the matrix P(EO/PO), earlier reported by DSC measurements[26] or ab initio calculations,[27] was from 4 to 6, and a state of saturation at high salt concentrations can, therefore, be envisaged as reflected in our results.

DSC thermograms of the PMMA/EMITFSI electrolytes and EMITFSI bulk (C = 2.56 mol kg^{-1}) at the heating scans are shown in the Supporting Information, 2. The EMITFSI bulk showed a sharp endothermic peak in the DSC thermogram, corresponding to the melting point of −16 °C. The endothermic peak disappears in the PMMA/EMITFSI electrolytes, and similar to the behavior of the P(EO/PO)/ LiTFSI electrolytes, only one T_g could be observed for the PMMA/EMITFSI electrolytes at all salt concentrations, which is indicative of compatibility of EMITFSI with the PMMA network polymer in the system. At all the concentrations, the PMMA/EMITFSI electrolytes are single-phase materials, and can be in a rubbery state at temperatures higher than the T_g. In contrast to the P(EO/PO)/LiTFSI electrolytes, the extent of total heat capacity change corresponding to the glass transition for the PMMA/EMITFSI electrolytes was found to increase with increasing EMITFSI concentration.

The T_g for the PMMA/EMITFSI electrolytes has been plotted against salt concentration in Figure 3, with the values listed in Table 2. The increase in salt concentration resulted in the monotonic decrease in the T_g, and the value approached that of the bulk EMITFSI at high salt concentrations. The interpretation

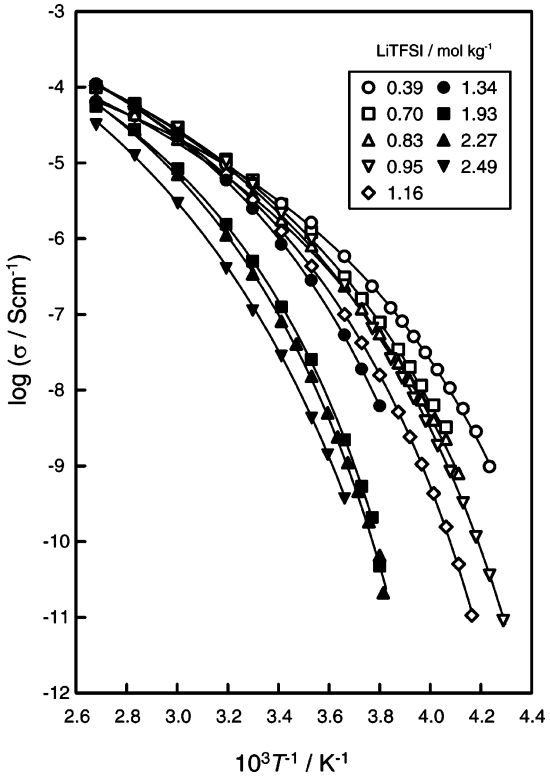

Figure 4. Arrhenius plots of ionic conductivity for P(EO/PO) network polymers containing LiTFSI.

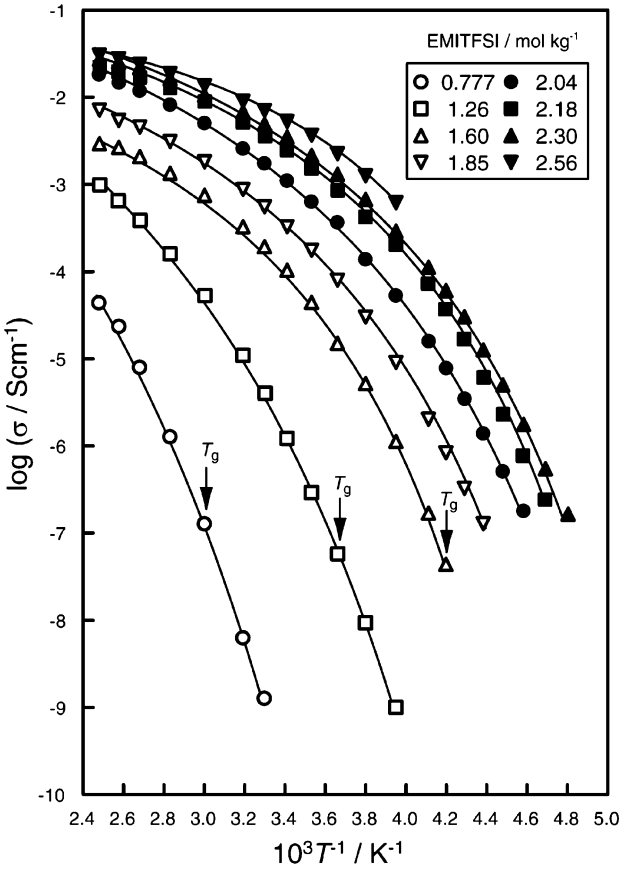

Figure 5. Arrhenius plots of ionic conductivity for PMMA network polymers with dissolved EMITFSI.

of results of the T_g for the binary system of PMMA/EMITFSI, by free volume consideration[28a] or additivity of weight fraction,[28b] shows the system to be a completely compatible one.[14]

The changes in the magnitude of the T_g under the identical scale of salt concentration for the two systems are compared. In the concentration range studied, the maximum change in the T_g for the P(EO/PO)/LiTFSI electrolytes upon the addition of LiTFSI is ca. 40 K (Figure 3), but a significant change of ca. 180 K (Figure 5) can be observed for the PMMA/EMITFSI electrolytes upon the addition of EMITFSI in PMMA. The difference may be attributed to the fact that the difference in the T_g for P(EO/PO) (with a lower T_g) and LiTFSI (with a higher T_g) is smaller than that of PMMA (with a higher T_g) and EMITFSI (with a lower T_g). The linear increase in the T_g with increasing salt concentration for the P(EO/PO)/LiTFSI system is mainly due to the ion−dipole interaction of the lithium cation with the polyether oxygen, which may act as a transient cross-linking point in the polymer electrolytes. LiTFSI (mp 230 °C) also has strong ion−ion interaction in the polyether between the anion and the cation, to which the ether oxygen ligands are coordinated. In contrast, EMITFSI, which has a low melting point (mp −16 °C) and consists of a cation with low Lewis acidity and an anion with low Lewis basicity, should have much weaker ion−ion interaction than LiTFSI. The ion−dipole interaction between EMITFSI and PMMA also appears to be weaker than that between LiTFSI and P(EO/PO), since the EMITFSI functions as a plasticizing salt toward PMMA, resulting in a decrease in the T_g with the addition of EMITFSI in the PMMA/EMITFSI electrolytes. These considerations are supported by the fact that LiTFSI dissociation is facilitated by the solvation with the matrix P(EO/PO), whereas EMITFSI, being an ionic liquid, has a self-dissociation property[8a] even in the absence of the interaction with PMMA.

The extent of heat capacity change during glass transition defines the behavior of structural relaxation time, and *fragility* is a measure of how rapidly the structure changes with increasing temperature above the T_g.[20−23] For a *fragile* system, the heat capacity of a liquid near the T_g is much higher than that of its glass, implying that the structure changes rapidly with temperature. Conversely, the structure of a *strong* system resists thermal change, and the change in heat capacity at the glass transition is much smaller. The wide difference in the extent of heat capacity change, depending on the systems and salt concentration (Supporting Information, 1 and 2), indicates that the concept of strong/fragile seems to be applicable to the polymer electrolytes (vide infra).

Ionic Conductivity. Figure 4 depicts the temperature dependence of the ionic conductivity (σ) for the network polymer electrolytes based on P(EO/PO) and LiTFSI. The σ for these electrolytes is on the order of 10^{-6} S cm^{-1} at 30 °C. The σ at low temperatures has been found to decrease with increasing salt concentration. The extent of the change in the σ was not so prominent at high temperatures.

The temperature dependence of ionic conductivity for network polymer electrolytes based on PMMA and EMITFSI along with that for bulk EMITFSI ($C = 2.56$ mol kg^{-1}) is shown in Figure 5. The σ increases monotonically with salt concentration. At high salt concentrations, high ionic conductivity close to 10^{-2} S cm^{-1} at 30 °C can be attained, which is more than 100 times higher than the values ever reported for polymer electrolytes at ambient temperature. The high ionic conductivity of the PMMA/EMITFSI ion gels is mainly attributable to the high ionic conductivity of EMITFSI itself, that is, the self-dissociating and ion transporting abilities. However, ionic species in ionic liquids have been found to form ion aggregates and ion clusters.[8] For the PMMA/EMITFSI system, the interaction of the PMMA matrix especially with the $TFSI^-$ anion has been found to

prohibit the formation of ion clusters or associates from the pulsed-field-gradient spin−echo NMR measurements, which also leads to enhanced ionic conductivity due to an increase in the number of carrier ions in the ion gels.[14]

The Arrhenius plots of ionic conductivity for both of the systems exhibit positively curved profiles, necessitating further interpretation of the results by either the Williams−Landel−Ferry (WLF) or the Vogel−Tamman−Fulcher (VTF) equation. We applied the VTF equation for ionic conductivity[29]

$$\sigma = AT^{-1/2} \exp[-B/(T - T_0)] \quad (1)$$

where A is a preexponential constant proportional to the number of carrier ions, B is the pseudoactivation energy for conduction, and T_0 is the ideal glass transition temperature, in other words, the temperature at which free volume or configurational entropy becomes zero and ionic conduction is completely frozen. In this study, we have measured the ionic conductivity values for both polymer electrolytes over a wide temperature range, with the lowest temperature being close to or in some cases below the T_g, in contrast to the literature, where conductivities are usually reported at higher temperatures, at least well above the T_g. The best-fit parameters for the experimental results have been tabulated in Tables 1 and 2 for the P(EO/PO)/LiTFSI and PMMA/EMITFSI systems, respectively. Since the conductivity data over the wide temperature range were used for the fitting to eq 1, we expect the fitting parameters to provide a more meaningful and reliable interpretation of our results. The parameter B is found to increase with increasing concentration of LiTFSI for the P(EO/PO)/LiTFSI system, whereas the PMMA/EMITFSI system shows a reverse trend with increasing EMITFSI concentration. In addition, the parameter A increases with concentration for the P(EO/PO)/LiTFSI system, whereas the PMMA/HTFSI system does not show such a trend.

Difference between the T_g and T_0 and Conductivity at the T_g. The T_0 values obtained by the VTF fittings are plotted in Figures 2 and 3 for the P(EO/PO)/LiTFSI and PMMA/EMITFSI electrolytes, respectively.

In the P(EO/PO)/LiTFSI system, the T_g and T_0 shift in parallel with a change in LiTFSI concentration (Figure 2), maintaining almost the regular difference of ca. 40−50 °C. This is in good agreement with the interpretations based on the WLF and VTF equations ($T_g - T_0 = 51.6$ °C), which are rationalized by the free volume and configurational entropy models for conventional polymer electrolytes. In the P(EO/PO)/LiTFSI system, the lithium cation is considered to be captured by the P(EO/PO) oxygen atoms, and the ionic conduction occurs with relaxation motion of the P(EO/PO) segment. This is why the T_g and T_0 have closer values, indicating that the ionic motion is frozen when the system is in the glassy state. In other words, the ionic motion is *coupled* with the segmental motion of the P(EO/PO) chain.

In contrast to that for the P(EO/PO)/LiTFSI system, the difference between the T_g and T_0 increased with decreasing salt concentration (Figure 3) for the PMMA/EMITFSI system. The T_g and T_0 are close together for the EMITFSI bulk ($C = 2.56$ mol kg^{-1}); however, the difference in the EMITFSI concentration range studied reaches up to 100 °C. The large difference means that the ions in the system can be mobile even at the T_g, indicating that the ionic motion is *decoupled* from the structural relaxation.

According to the conventional free volume theory,[30] the fractional free volume (v_f) in amorphous polymers has the same value (0.025) and increases linearly with $T - T_g$. The ionic conductivities for both of the systems at the T_g ($\sigma(T_g)$) have, therefore, been analyzed to provide further insight into the ion transport processes involved in the polymer electrolytes. The $\sigma(T_g)$ for the polymer electrolytes was obtained either experimentally or from the extrapolation of the temperature dependence of ionic conductivity curves using the VTF equation. Figure 6 shows the $\sigma(T_g)$ plotted as a function of salt concentration. The $\sigma(T_g)$ for the P(EO/ PO)/LiTFSI electrolytes was on the order of 10^{-14}−10^{-13} S cm^{-1} and increased with increasing salt concentration. Since the T_g is an iso free volume state, as mentioned above, the gradual increase in the conductivity seems to reflect the increase in the number of carrier ions. This consideration is also supported by the phenomenon of attaining a limiting value for $\sigma(T_g)$ with increasing salt concentration, where ion-pairing may proceed with concentration. In the P(EO/PO)/LiTFSI electrolytes, the ions can be appreciably mobile with the segmental motion due to the strong ion−dipole interaction, and the free volume necessary for the ionic motion is dominated by that for the segmental motion. In sharp contrast, the $\sigma(T_g)$ for the PMMA/EMITFSI electrolytes reaches 10^{-7} S cm^{-1} when the concentration of PMMA is high. As shown in Figure 5, the $\sigma(T_g)$ was measurable by our experimental setup for the high PMMA concentration electrolytes. Also, the $\sigma(T_g)$ for the PMMA/EMITFSI electrolytes greatly changes, ranging from 10^{-14} to 10^{-7} S cm^{-1}. When the concentration of EMITFSI is high, the ion transport property seems to be dominated by that of EMITFSI itself, and thus, at the T_g, the ionic transport diminishes due to the glass formation. However, with decreasing EMITFSI concentration, EMITSI becomes a minor component of the binary system. Since EMITFSI has a self-dissociation property and weakly interacts with the PMMA chain, the constituted ions seem to be mobile by themselves even at the T_g, not associating with the segmental motion as in the case of the P(EO/PO)/LiTFSI electrolytes. The fractional free volume at the T_g is the critical free volume for segmental motion of polymers. If the critical free volume for ionic motion is much smaller than that of the segmental motion, which seems to be the case for the PMMA/EMITFSI electrolytes due to the weak ion−polymer interaction as well as the self-dissociation property, the ions may be mobile even at the T_g.

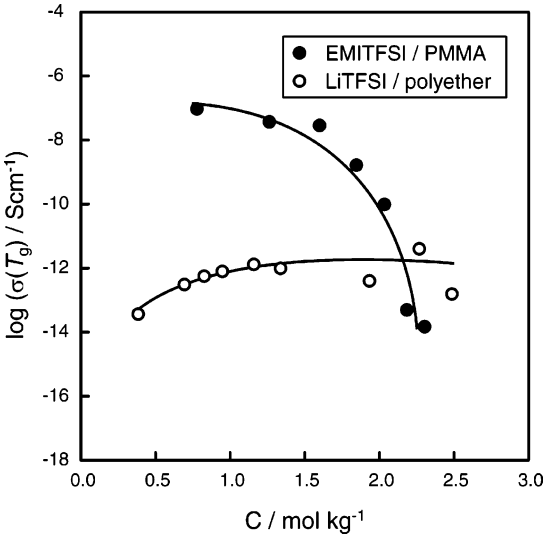

Figure 6. Ionic conductivity at the T_g ($\sigma(T_g)$) for PMMA/LiTFSI and P(EO/PO)/LiTFSI polymer electrolytes.

The $\sigma(T_g)$ values can be used for the approximation of the decoupling index (R_τ), which is defined as the ratio of the conductivity relaxation time (τ_σ) to structural relaxation time (τ_s), using the relationship[20]

$$\log R_\tau \approx 14.3 + \log \sigma(T_g) \quad (2)$$

The log R_τ value for P(EO/PO)/LiTFSI and PMMA/EMITFSI electrolytes ranges from 0.3 to 1.3 and from 0.3 to 7.3, respectively. A high value of R_τ means the ionic motion is only weakly controlled by the immobile elements of the structure, meaning that the conductivity is highly decoupled from the segmental motion of the polymer chains.[20] This further clarifies the phenomenon of coupling/decoupling in the systems.

***T*g-Normalized Temperature Dependency of Conductivity**. In the case of the P(EO/PO)/LiTFSI electrolytes, despite a wide variation in the concentration of the carrier species, the Arrhenius plots of ionic conductivity normalized by the T_g can be approximated by a master curve, as shown in Figure 7. The σ diminishes more and more rapidly when T_g is approached and follows the VTF equation with $\sigma(T_g) = 10^{-14}-10^{-13}$ S cm^{-1} (fragile system).[23] The ion conduction for the P(EO/PO)/LiTFSI electrolytes is, hence, governed by the glass transition of the system, and the σ primarily depends on the number of charge carriers at the T_g.

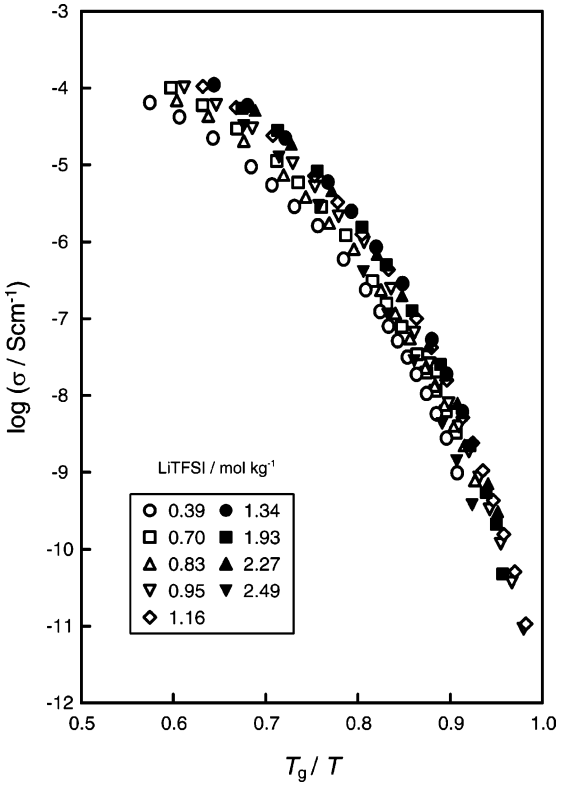

Figure 7. T_g-scaled Arrhenius plots of ionic conductivity for P(EO/PO) network polymers containing LiTFSI.

Figure 8 shows the ionic conductivities normalized by the T_g for the PMMA/EMITFSI electrolytes. At high salt concentrations, the σ decreased exponentially in the proximity of the T_g. This indicates the systems at high EMITFSI concentrations to be fragile. Attention should be focused on the σ at low salt concentrations, where the decrease in the σ when the T_g is appoached becomes much less pronounced (strong system),[23] compared with that of the PMMA/EMITFSI electrolytes with high EMITFSI concentrations and of the P(EO/PO)/LiTFSI electrolytes. This anomaly is well consistent with the high values of the $\sigma(T_g)$ at these concentrations. By increasing the polymer content in the PMMA/EMITFSI electrolytes, a change from a *coupling*/*fragile* system to a *decoupling*/*strong* system might occur in the electrolytes.

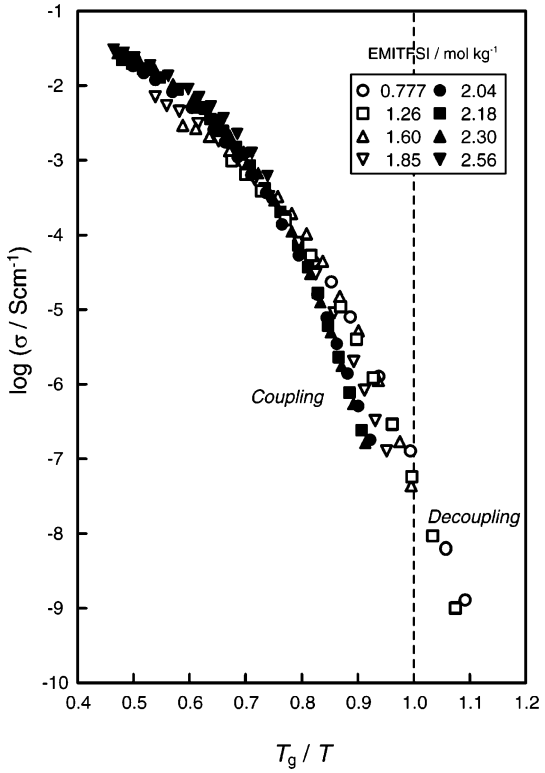

Figure 8. T_g-scaled Arrhenius plots of ionic conductivity for PMMA network polymers with dissolved EMITFSI.

Concluding Remarks

By comparing the calorimetric and conductometric results of a conventional polymer electrolyte based on LITFSI incorporated into a soft polyether matrix and an ion gel based on an ionic liquid (EMITFSI) incorporated into a hard polymer matrix (PMMA), we obtained a broad picture of the physicochemical processes involved in ionic transport in the polymer electrolytes. The conventional polyether electrolyte is a *coupling* system, and the relaxation time for the segmental motion is coupled with the conduction relaxation time. The ion transport behavior of the ion gels, on the other hand, varies depending on the concentration. A change from a coupling/fragile to a decoupling/strong system is apparent with decreasing salt concentration in the ion gels.

Acknowledgment. This research was supported in part by Grants-in-Aid for Scientific Research (Nos. 14350452 and 16205024) from the MEXT and CREST-JST. We are grateful to Dai-ichi Kogyo Seiyaku Co., Ltd. for the generous supply of some of the reagents. M.A.B.H.S. and H.T. also acknowledge JSPS for financial support.

Supporting Information Available: DSC thermograms of P(EO/PO) network polymers with varying amounts of LiTFSI and of PMMA network polymers with varying amounts of dissolved EMITFSI and EMITFSI bulk at a heating rate of 10 °C min^{-1} (PDF). This material is available free of charge via the Internet at http://pubs.acs.org.

References and Notes

(1) *Applications of Electroactive Polymers*; Scrosati, B., Ed.; Chapman & Hall: London, 1993.

(2) *Polymer Electrolyte Reviews 1 and 2*; MacCallum, J. R., Vincent, C. A., Eds.; Elsevier Applied Science: London, 1987 and 1989.

(3) Gray, F. M. *Solid Polymer Electrolytes*; VCH Publishers: New York, 1991.

(4) (a) Nishimoto, A.; Watanabe, M.; Ikeda, Y.; Kohjiya, S. *Electrochim. Acta* **1998**, *43*, 1177. (b) Nishimoto, A.; Agehara, K.; Furuya, N.; Watanabe, T.; Watanabe, M. *Macromolecures* **1999**, *32*, 1541. (c) Watanabe, M.; Endo, T.; Nishimoto, A.; Miura, K.; Yanagida, M. *J. Power Sources* **1999**, *81*−*82*, 786.

(5) (a) Watanabe, M. In *Soild State Ionics: Materials and Applications*; Chowdari, B. V. R., Chandra, S., Singh, S., Srivastava, P. C., Eds.; World Scientific: Singapore, 1992; pp 149−157. (b) Angell, C. A.; Liu, C.; Sanchez, E. *Nature* **1993**, *362*, 137. (c) Watanabe, M.; Yamada, S.; Sanui, K.; Ogata, N. *J. Chem. Soc., Chem. Commun.* **1993**, 929. (d) Fan, J.; Angell, C. A. *Electrochim. Acta* **1995**, *40*, 2397.

(6) (a) Forsyth, M.; Sun, J.; McFarlane, D. R. *Solid State Ionics* **1998**, *112*, 161. (b) Ferry, A.; Edman, L.; Forsyth, M.; McFarlane, D. R.; Sun, J. *J. Appl. Phys.* **1999**, *86*, 2346.

(7) Wilkes, J. S.; Zaworotko, M. J. *J. Chem. Soc., Chem. Commun.* **1992**, 965.

(8) (a) Noda, A.; Hayamizu, K.; Watanabe, M. *J. Phys. Chem. B* **2001**, *105*, 4603. (b) Tokuda, H.; Hayamizu, K.; Ishii, K.; Susan, M. A. B. H.; Watanabe, M. *J. Phys. Chem. B* **2004**, *108*, 16593.

(9) *Ionic Liquids in Synthesis*; Wasserscheid, P., Welton, T., Eds.; Wiley-VCH Verlag: Weinheim, Germany, 2003.

(10) Watanabe, M.; Yamada, S.; Ogata, N. *Electrochim. Acta* **1995**, *40*, 285.

(11) (a) Noda, A.; Watanabe, M. *Electrochim. Acta* **2000**, *45*, 1265. (b) Watanabe, M.; Mizumura, T. *Solid State Ionics* **1996**, *86*−*88*, 385.

(12) (a) Scott, M. P.; Brazel, C. S.; Benton, M. G.; Mays, J. W.; Holbrey, J. D.; Rogers, R. D. *Chem. Commun.* **2002**, 1370. (b) Scott, M. P.; Rahman, M.; Brazel, C. S. *Eur. Polym. J.* **2003**, *39*, 1947.

(13) (a) Carlin, R. T.; Delong, H. C.; Fuller, J.; Trulove, P. C. *J. Electrochem. Soc.* **1994**, *141*, L73. (b) Carlin, R. T.; Fuller, J. *Chem. Commun.* **1997**, 1345. (c) Fuller, J.; Breda, A. C.; Carlin, R. T. *J. Electrochem. Soc.* **1997**, *144*, L67. (d) Fuller, J.; Breda, A. C.; Carlin, R. T. *J. Electroanal. Chem.* **1998**, *45*, 29.

(14) Susan, M. A. B. H.; Kaneko, T.; Noda, A.; Watanabe, M. *J. Am. Chem. Soc.*, in press.

(15) (a) Susan, M. A. B. H.; Noda, A.; Watanabe, M. In *ACS Symposium Series: Ionic liquids in Polymer System: Solvents, Additives, and Novel Applications*; Brazel, C. S., Rogers, R. D., Eds.; in press (b) Freemantle, M. *Chem. Eng. News* **2004**, *82* (18, May 3), 26.

(16) (a) Susan, M. A. B. H.; Noda, A.; Mitsushima, S.; Watanabe, M. *Chem. Commun.* **2003**, 938. (b) Noda, A.; Susan, M. A. B. H.; Kudo, K.; Mitsushima, S.; Hayamizu, K.; Watanabe, M. *J. Phys. Chem. B* **2003**, *107*, 4024. (c) Susan, M. A. B. H.; Yoo, M.; Nakamoto, H.; Watanabe, M. *Chem. Lett.* **2003**, *32*, 836. (d) Susan, M. A. B. H.; Nakamoto, H.; Yoo, M.; Watanabe, M. *Trans. Mater. Res. Soc. Jpn.* **2004**, *29*, 1043.

(17) Shoubukawa, H.; Tokuda, H.; Tabata, S.; Watanabe, M. *Electrochim. Acta* **2004**, *50*, 305.

(18) (a) Kawano, R.; Watanabe, M. *Chem. Commun.* **2003**, 330. (b) Kawano, R.; Matsui, H.; Matsuyama, C.; Sato, A.; Susan, M. A. B. H.; Tanabe, N.; Watanabe, M. *J. Photochem. Photobiol., A* **2004**, *164*, 87.

(19) (a) Angell, C. A. *Solid State Ionics* **1983**, *9*, *10*, 3. (b) Angell, C. A. *Solid State Ionics* **1986**, *18*, *19*, 72. (c) Videa, M.; Angell, C. A. *J. Phys. Chem. B* **1999**, *103*, 4185.

(20) (a) Angell, C. A. *Annu. Rev. Phys. Chem.* **1992**, *43*, 693. (b) Xu, W.; Wang, L.-M.; Angell, C. A. *Electrochim. Acta* **2003**, *48*, 2037.

(21) Debenedetti, P. G.; Stillinger, F. H. *Nature* **2001**, *410*, 259.

(22) Imrie, C. T.; Ingram, M. D.; Mchattie, G. S. *J. Phys. Chem. B* **1999**, *103*, 4132.

(23) (a) Bohmer, R.; Senapati, H.;, Angell, C. A. *J. Non-Cryst. Solids* **1991**, *131*−*133*, 182. (b) Angell, C. A. *J. Phys. Chem. B* **1993**, *97*, 6339. (c) Bohmer, R.; Ngai, K. L.; Angell, C. A.; Plazek, D. J. *J. Chem. Phys.* **1993**, *99*, 4201. (d) Angell, C. A. *Science* **1995**, *267*, 1924. (e) Speedy, R. J. *J. Phys. Chem. B* **1999**, *103*, 4060. (e) Ferrer, M. L.; Sakai, H.; Kivelson, D.; Alba-Simionesco, C. *J. Phys. Chem. B* **1999**, *103*, 4191. (f) Green, J. L.; Ito, K.; Xu, K.; Angell, C. A. *J. Phys. Chem. B* **1999**, *103*, 3991. (g) Martinez, L.-M.; Angell, C. A. *Nature* **2001**, *410*, 663.

(24) Bonhôte, P.; Dias, A.-P.; Papageorgiou, N.; Kalyanasundaram, K.; Grätzel, M. *Inorg. Chem.* **1996**, *35*, 1168.

(25) (a) Kono, M.; Hayashi, E.; Watanabe, M. *J. Electrochem. Soc.* **1999**, *146*, 1626. (b) Kono, M.; Hayashi, E.; Nishiura, M.; Watanabe, M. *J. Electrochem. Soc.* **2000**, *147*, 2517.

(26) Hsien, W. C.; Feng, C. C. *Polymer* **2001**, *42*, 9763.

(27) (a) Johanson, P.; Tegenfeldt, J.; Lindgren, J. *Polymer* **1999**, *40*, 4399. (b) Johanson, P. *Polymer* **2001**, *42*, 4367.

(28) (a) Gordon, M.; Taylor, J. S. *J. Appl. Chem.* **1952**, *2*, 493. (b) Fox, T. G. *Bull. Am. Phys. Soc.* **1956**, *1*, 123.

(29) (a) Vogel, H. *Phys. Z.* **1921**, *22*, 645. (b) Fulcher, G. S. *J. Am. Ceram. Soc.* **1923**, *8*, 339.

(30) Cohen, M. H.; Turnbull, D. *J. Chem. Phys.* **1959**, *31*, 1164.